Design and performance of a novel vacuum-capable terahertz time-domain spectrometer

Y. C. Shen, P. Upadhya, E. H. Linfield, and A. G. Davies

Abstract—**We have designed and built a vacuum-capable terahertz (THz) time-domain spectrometer which allows THz spectroscopy measurements to be made whilst avoiding interference from, for example, water vapour absorption. Using a biased semi-insulting GaAs emitter and a 1-mm-thick (110) oriented ZnTe crystal as an electro-optic detection sensor, we achieved a dynamic range of over 10^{10} in THz power and a useful frequency range of over 3 THz. The system is very stable with a <2% day-to-day spectral variation, and up to ten samples can be measured without the need to open the vacuum chamber. In addition, the broadband (over 30 THz) capability of the system has been demonstrated by using a 30 μm GaSe crystal as the emitter and a 20 μm ZnTe crystal as the detector. The fine absorption features of uric acid were resolved at room temperature with this spectrometer, and are also presented.**

Index Terms—**terahertz spectroscopy, time-domain, vacuum**

I. INTRODUCTION

OVER recent years, there has been a growing interest in terahertz (THz) time-domain spectroscopy and its application to the study of biological systems [1]. This spectroscopy provides a direct measurement of the THz electric field which, upon Fourier transformation, yields both amplitude and phase information which is very convenient for studying the real and imaginary parts of dielectric functions. In fact, the rotational and vibrational spectra of many liquids and gases lie within the THz frequency range [2].

Unfortunately, in the THz range, the measured spectra often show strong absorption features resulting from the gases present in the atmosphere, principally water vapour. Although purging the spectrometer with nitrogen can diminish these interfering absorption features, a vacuum-capable THz spectrometer provides better and cleaner spectra, which is of great advantage for biological applications. Here we report on the design and performance of a vacuum-capable THz time domain spectrometer.

To perform THz generation and detection in vacuum, care has to been taken to choose the appropriate THz emitter and detector in order to minimize the effect of vibrations associated with pumping, and components moving under evacuation in the confined environment. In our system, ZnTe crystal electro-optic sensors [3–5] were employed for THz detection because they require neither silicon lenses nor the related coupling media. For THz generation, two methods are commonly used. One is based on optical rectification in which frequency components present in the bandwidth of an ultrashort near-infrared/visible laser pulse are mixed in a nonlinear crystal such as ZnTe or GaSe [5,6]. In the second method, an ultrashort near-infrared/visible laser pulse illuminates a semiconductor such as GaAs, biased with an electric field, giving rise to a fast current transient which emits a THz pulse [7-9]. Here we principally used a semi-insulating GaAs (SI-GaAs) emitter biased with an ac square wave, although a GaSe crystal was also used to investigate the broadband capability of our vacuum-capable THz time domain spectrometer.

II. EXPERIMENT

A diode-laser-pumped titanium sapphire laser was used to generate 12 fs laser pulses centered at 790 nm, with a 100 nm bandwidth and a repetition rate of 80 MHz. The 200 mW laser spot of diameter 200 μm was focused onto the surface of the semiconductor emitter. We used a simple semiconductor emitter comprising a SI-GaAs substrate and two vacuum-deposited NiCr/Au electrodes with a 400μm separation. The relatively wide gap and large laser spot size provides a powerful (over 10 μW) and stable THz emitter, which is not sensitive to possible vibrations or any long-term instabilities in the laser beam. The THz pulses generated are collimated and focused onto the sample by a pair of parabolic mirrors, with a factor of four magnification. The transmitted THz pulse is then collected by another pair of parabolic mirrors and focused onto a ZnTe crystal for electro-optic detection.

The prominent feature of our experimental system is that the

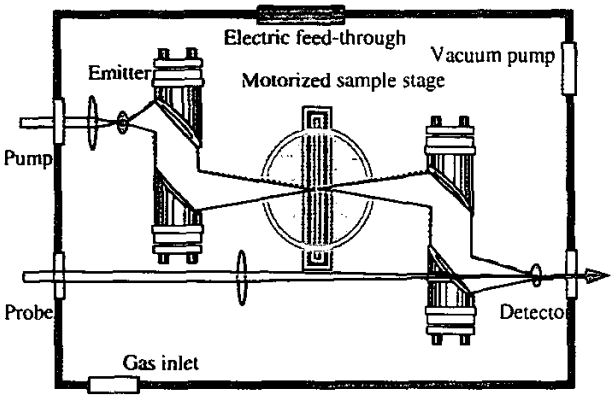

Fig. 1 Schematic representation of THz generation and detection inside the vacuum chamber; refer to text for further details.

Y. C. Shen, P. Upadhya, E. H. Linfield, and A. G. Davies are with the Cavendish Laboratory, University of Cambridge, Madingley Road, Cambridge CB3 0HE, UK (email: ys244@cam.ac.uk). This work was supported by the EPSRC, the Royal Society, and Toshiba Research Europe Ltd.

0-7803-7630-7/02/$17.00©2002 IEEE

THz generation and detection components are enclosed in a vacuum box, providing vacuum levels as low as 10^{-5} mbar. The samples are mounted on a motorized stage which allows up to ten samples to be measured without the need to open the vacuum chamber. This is particularly important for medical applications where a large number of samples need to be measured quickly. Fig. 1 shows the schematic arrangement of the spectrometer. The gas inlet is used for dry-nitrogen purging when vacuum pumping is not necessary. It can also introduce trace gases into the spectrometer for measurement. The electrical feed-through provides the square-wave ac bias voltage to the GaAs emitter. A further 25 pin electrical feed-through is used to control the motorized stage.

All the optic components inside the vacuum chamber are mounted on a separate optic plate. The plate is supported at the four corners of the vacuum chamber, where the pressure-related deformation is minimum. This design minimizes the effect of the possible bending of the vacuum chamber wall owing to the enormous atmosphere pressure. No change in the measured THz signal was observed during or after vacuum pumping, proving the effectiveness of the design.

III. RESULTS AND DISCUSSIONS

A. *THz signal*

Fig. 2 shows typical time-domain THz signals generated by a SI-GaAs emitter and measured with ZnTe crystal electro-optic sensors. The full-width-at-half-maximum (FWHM) of the pulses were determined to be 0.38 ps and 0.30 ps for the THz pulses measured with 1 mm and 0.2-mm-thick-ZnTe-crystals, respectively. The second peak (shoulder) at around 3.2 ps of curve (1) in Fig 2 (a), which is more pronounced in curve (2), is a result of the dispersion of the THz pulse in the SI-GaAs emitter and the ZnTe detector. This shoulder appears only when the signal has sufficient high frequency components, providing a good indication as to whether the system is well aligned. The second pulse of curve (2) around 7 ps comes from the reflection of the THz pulse at the surfaces of the ZnTe crystal. A similar pulse also appears in curve (1) but at a much later time (20 ps) owing to the different crystal thickness.

The amplitude of the THz pulse measured with the 1-mm-thick ZnTe crystal is only about twice as large as that measured with the 0.2 mm crystal, instead of the five-fold increase one might expect if the sensitivity were simply proportional to the crystal thickness. This is a result of phenomena associated with absorption and phase matching in the ZnTe crystal. As reported by Gallot *et al.* [10], ZnTe has strong absorption around the two phonon lines at 1.6 and 3.7 THz, in addition to the strong transverse-optic phonon line at 5.3 THz. Although increasing the crystal thickness will increase the detection sensitivity, it will also increase both the absorption and the effects of phase mismatch between the THz and near-infrared beams. These, in turn, reduce both the effective sensitivity and the bandwidth of the electro-optic detection process.

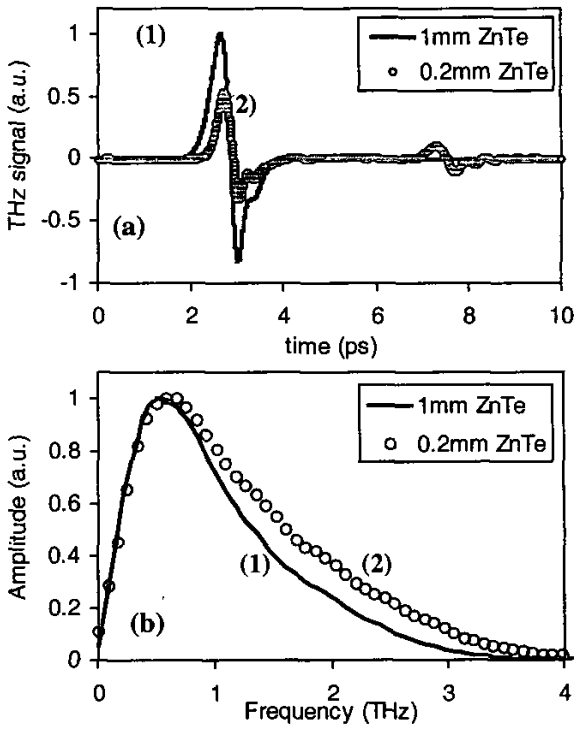

Fig. 2 (a) Temporal waveform and (b) spectra of the THz pulse generated from a SI-GaAs emitter and measured with a ZnTe crystal electro-optic sensor. The thickness of the sensor is 1 mm (solid line) and 0.2mm (open circle). Note that the spectra were normalized to one for comparison.

The Fourier transforms of the measured THz signals peak at 0.7 THz and have useful frequency components over 3 THz, as shown in Fig. 2. More bandwidth was obtained with a 0.2-mm-thick crystal. However, considering the absolute amplitude, the 1-mm-thick crystal still provides better performance in the frequency range of 0.2 – 2.6 THz.

The bandwidth of the THz spectrometer is determined by the frequency response of the ZnTe crystal and the bandwidth of

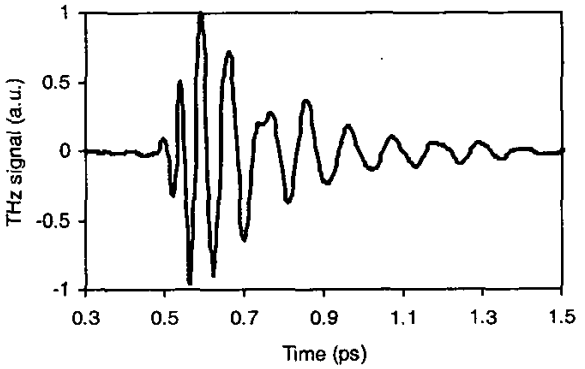

Fig. 3 THz transient generated in a 30mm thick GaSe crystal by optical rectification of 12fs laser pulse at a 48° phase matching angle, detected with a 20mm thick ZnTe electro-optic sensor. The Fourier transform of this signal has frequency components above 30THz.

the THz waveform generated from the biased semiconductor. In addition, owing to the extreme bandwidth, with a frequency range covering 1 – 2 orders of magnitude, the optical system may also play an important role in shaping the THz signal. In order to clarify the effect of this, we replaced the SI-GaAs antenna with a 30-μm-thick GaSe crystal as the emitter and used a 20-μm-thick ZnTe crystal as the detector. GaSe crystal has been shown to be a very good material for generating broad-bandwidth THz radiation by phase-matched optical rectification of the fs laser pulses [5]. The measured THz pulses shown in Fig.3 have a FWHM of 20 fs. The Fourier transform of this signal has frequency components of over 30 THz, indicating that the optical system employed here for is not a limiting factor for the bandwidth of the spectrometer.

In addition, once generated, the THz pulses propagate about 500 mm before reaching the ZnTe detector, and will be reshaped owing to the absorption and dispersion of the pulses in the propagating media. The vacuum chamber minimizes such effects.

B. Signal-to-noise ratio

The absorption of biomolecules in the THz frequency range arises from the molecular rotational and vibrational modes, as well as intermolecular interactions. The absorption is normally small in comparison with absorption in the mid-IR, which arises from covalent bond vibrations. High signal-to-noise ratio and/or large dynamic range are thus essential to resolve the small absorption features.

The noise level and the signal amplitude are two important factors determining the achievable signal-to-noise ratio. The frequency dependence of the signal noise was measured by sweeping the chopper frequency from 100 Hz to 100 kHz. Below 500 Hz the noise is high, possibly owing to the fact that the electro-optic detection scheme is sensitive to low frequency vibrations. Above 1 kHz, one is mainly limited by quantum noise in the probe laser beam. It should be pointed out that a balanced photodiode detection scheme is essential to achieve the quantum noise limit. The noise level was found to be at least one order of magnitude higher when the two photodiodes were not balanced.

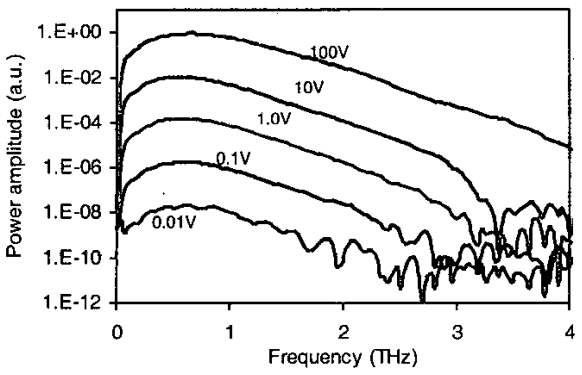

Fig. 4 THz power spectra measured using 1 mm thick ZnTe crystal. From top to bottom, the biased voltage on the GaAs emitter are 100V, 10V, 1.0V, 0.1V and 0.01V.

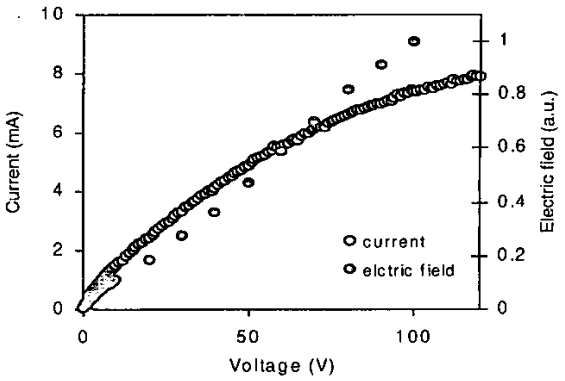

Fig. 5 Measured THz peak amplitude (solid circle) and photocurrent (open circle) as a function of the applied bias voltage. A voltage of 100 V corresponds to a ±100V ac square wave.

The signal amplitude is mainly determined by the THz power generated in the biased semiconductor emitter, and then collected at the detector. The GaAs emitter employed in our spectrometer proved to be a powerful and stable source. Fig. 4 shows the power amplitude spectra obtained at different bias voltages. A dynamic range or signal-to-noise ratio of 10^{10} is clearly achievable in the measured THz power spectra. Fig. 5 shows the I–V curve of the GaAs emitter under 200 mW laser pulse illumination measured up to 100 V, together with the measured THz electric field. The electric field of the THz pulse increases linearly with applied voltage. We note that with a water cooling scheme, Zhao *et al.* [11] reported that over 300 V ac could be applied to a similar GaAs emitter without causing any damage. Owing to the limited dynamic range of our digital lock-in amplifier and also to minimize heating, our GaAs emitter was normally operated at 80 V, although no damage was found at biases up to 160 V.

C. Water vapor absorption

To demonstrate the vacuum capability of our THz spectrometer, sixty spectra were recorded at time intervals of one second during the vacuum pumping process, as shown in Fig. 6. In the frequency range 0.5 – 2.5 THz, twenty-eight

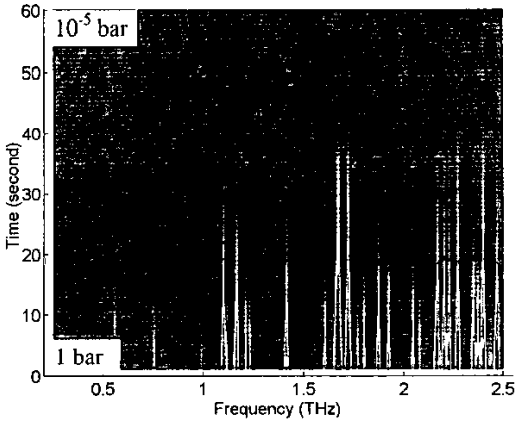

Fig. 6: 60 spectra recorded at a time interval of one second during the pumping process, measured with our vacuum capable THz spectrometer.

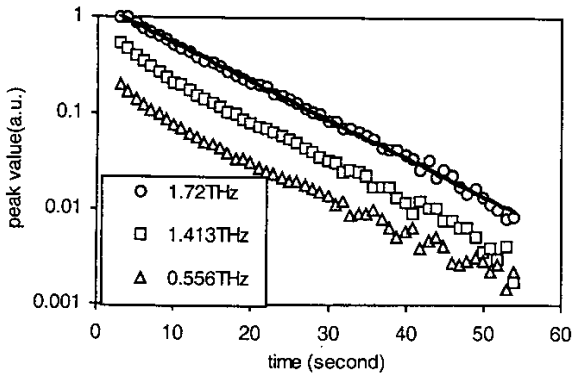

Fig. 7 The peak amplitude of the water vapour absorption at 0.556, 1.413 and 1.72THz are plotted as a function of pumping time.

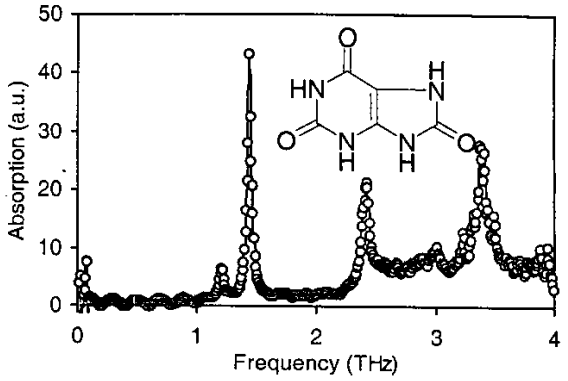

Fig. 8 THz spectrum of a uric acid pellet measured at room temperature using the vacuum capable THz time-domain spectrometer.

absorption lines are visible in the THz spectra before vacuum pumping. However, all the absorption lines were eliminated within one minute after switching on the vacuum pump. This is at least 20 times faster than with a nitrogen purging method.

For these measurements, the scan range of the optical delay stage was 10 mm, corresponding to a frequency resolution of 15 GHz. At this resolution the absorption lines were determined to be 0.558, 0.753, 0.990, 1.100, 1.115, 1.165, 1.210, 1.23, 1.323, 1.413, 1.663, 1.673, 1.718, 1.765, 1.798, 1.842, 1.87, 1.92, 2.02, 2.043, 2.078, 2.09, 2.165, 2.2, 2.225, 2.268, 2.345, 2.368, 2.395, and 2.465 THz. These values agree well with published data [12].

The water vapor absorption in the chamber can be expressed as $A = \exp[-\alpha L\, n(t)]$, where L is the THz path length, α is the molecular extinction coefficient, and $n(t)$ is the number density of water molecules in the chamber which decreases with time after the vacuum pump is switched on. The absorption peak amplitudes of the THz spectra at 0.556, 1.413, and 1.72 THz are plotted against time in Fig. 7, and we indeed observe that the water vapour absorption decreases exponentially with pumping time.

Finally, for completeness, the vacuum-capable THz time-domain spectrometer was applied to study uric acid, an important substance frequently encountered in clinical diagnosis. Uric acid was purchased from Sigma-Aldrich (product #51449) and used without further purification. Pellet samples were prepared by mixing together uric acid and polyethylene powder in a mass ratio of 1:1 and pressing into pellets with a manual pellet maker. We recorded sixty spectra of uric acid at time intervals of one second at room temperature during the evacuation process. The absorption features of uric acid were pronounced after the water vapour absorption was removed, as shown in Fig. 8. The small oscillations in the spectrum are due to an etalon effect owing to THz reflections at the pellet sample surfaces. It is interesting that uric acid has strong absorption features in the THz range at room temperature, including three major absorption peaks at 1.44, 2.41, and 3.40 THz. Two minor peaks at 1.21 and 3.01 THz were also resolved. The origin of these absorption peaks is a subject of further study.

ACKNOWLEDGMENT

We thank P. F. Taday of TeraView Ltd., M. Johnston and A. Dowd for helpful discussions.

REFERENCES

[1] S. W. Smye, J. M. Chamberlain, A. J. Fitzgerald and E. Berry, "The interaction between Terahertz radiation and biological tissue", *Phys. Med. Biol.*, vol. 46, no. 9, pp. R101–112, Sept. 2001, and the references therein.

[2] "Infrared and Raman spectroscopy, method and applications", ed. B. Schrader, VCH Verlagsgesellschaft mbH, (Weiheim, Germany), 1995.

[3] Q. Wu and X. -C. Zhang, "Free-space electro-optic sampling of THz beams", *Appl. Phys. Lett.*, vol. 67, no. 24, pp. 3523-3525, Dec. 1995.

[4] P. U. Jepsen, C. Winnewisser, M. Schall, V. Schyja, S. R. Keiding, and H.Helm, "Detection of THz pulses by phase retardation in lithium tantalite", *Phys. Rev. E*, vol. 53, iss. 4, pp. R3052, Apr. 1996.

[5] R. Huber, A. Brodschelm, F. Tauser, and A. Leitenstorfer, "Generation and field-resolved detection of femtosecond electromagnetic pulses tunable up to 41 THz", *Appl. Phys. Lett.*, vol. 76, no. 22, pp. 3191–3193, May 2000.

[6] X. -C. Zhang, Y. Yin, and X. F. Ma, "Coherent measurement of THz optical rectification from electro-optic crystals", *Appl. Phys. Lett.*, vol. 61, no. 23, pp. 2764-2766, Dec. 1992.

[7] M. van Exter and D. R. Grischkowsky, "Characterization of an optoelectronic terahertz beam system", *IEEE Trans. Microwave TheoryTech.*, vol. 38, no. 11, pp. 1684-1691, Nov. 1990.

[8] J. T. Darrow, B. B. Hu, X. -C. Zhang, and D. H. Auston, "Subpicosecond electromagnetic pulses from large-aperture photoconducting antennas", *Opt. Lett.*, vol. 15, no. 6, pp. 323-325, March 1990.

[9] P. U. Jepsen, R. H. Jacobsen and S. R. Keiding, "Generation and detection of terahertz pulses from biased semiconductor antennas", *J. Opt. Soc. Am. B*, vol. 13, no.1, pp. 2424–2436, Nov. 1996.

[10] G. Gallot, J. Zhang, R. W. McGowan, T. -I. Jeon, and D. Grischkowsky, "Measurements of the THz absorption and dispersion of ZnTe and their relevance to the electro-optic detection of THz radiation", *Appl. Phys. Lett.*, vol. 74, no. 23, pp. 3450–3452, June 1999.

[11] G. Zhao, R. N. Schouten, N. van der Valk, W. Th. Wenckebach, and P. C. M. Plankena, "Design and performance of a THz emission and detection setup based on a semi-insulating GaAs emitter", *Rev. Sci. Instrum.*, vol. 73, no. 4, pp. 1715-1719, Apr. 2002.

[12] R. A. Chevile and D. Grischkosky, "Far-infrared foreign and self-broadened rotational linewidths of high-temperature water vapor", *J. Opt. Soc. Am. B*, vol.16, no. 2, pp. 317–322, Feb. 1999.